Electronic Supplementary Material (ESI) for Physical Chemistry Chemical Physics.

Electronic Supplementary Information : A Theoretical Elucidation of Tuneable Fluorescence of a Full-color Emissive ESIPT Dye.

Pauline M. Vérité, Simon Hédé, Denis Jacquemin

Laboratoire CEISAM -UMR CNRS 6230,Université de Nantes, 2 Rue de la Houssinière, BP 92208, 44322 Nantes Cedex 3, France ; Tel.: +33-2-51-12-55-64 ; E-mail: Denis.Jacquemin@univ-nantes.fr

S1 ESIPT process

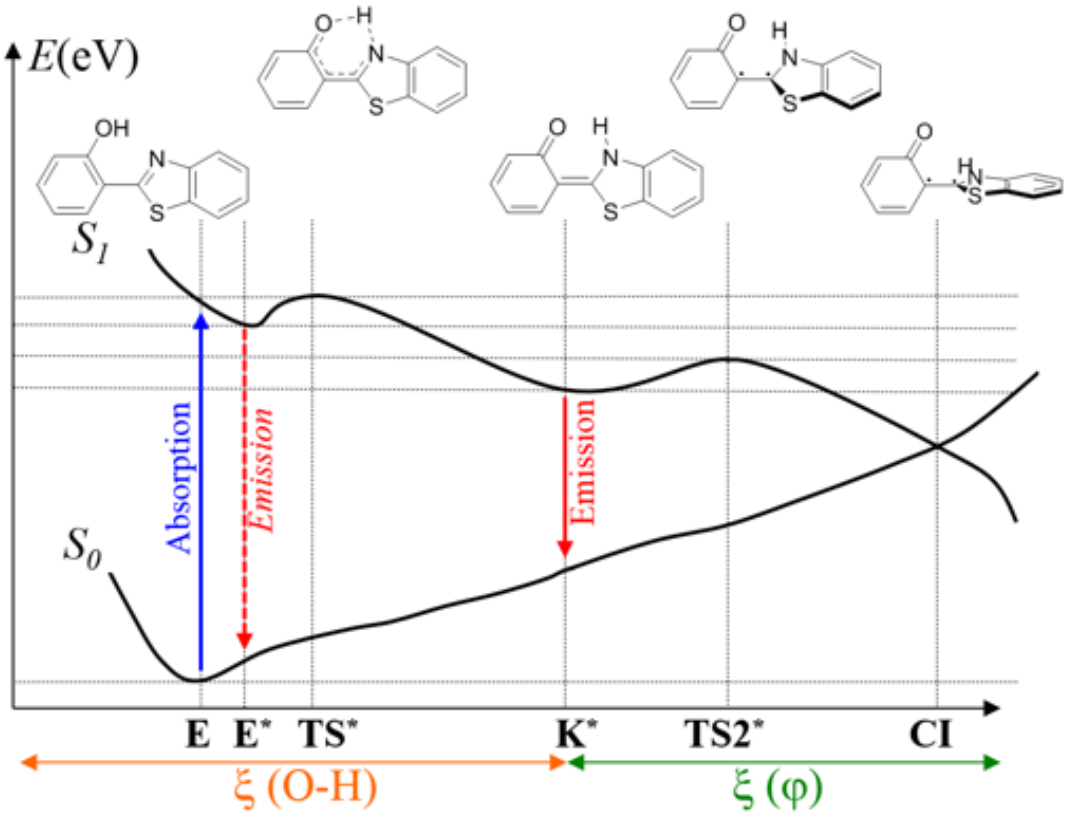

Figure S1: Representation of the potential energy surface during the ESIPT process, with first a proton transfer (O-H reaction coordinate) and next a twist of the structure leading to a conical intersection (CI), back to the ground-state.

S2 Results of calculations performed in 1,4-Dioxane (DOX)

S2.1 Ground state structure geometry

Bond length	Theoretical	Experimental[1]
1	1.740	1.625
2	0.993	0.996
3	1.345	1.355
4	1.409	1.403
5	1.394	1.388
6	1.392	1.390
7	1.390	1.383
8	1.402	1.396
9	1.411	1.414
10	1.470	1.474
11	1.371	1.375
12	1.391	1.396
13	1.379	1.380
14	1.371	1.384
15	1.321	1.329
16	1.475	1.471
17	1.298	1.308
18	1.379	1.380
19	1.407	1.399
20	1.738	1.736
21	1.770	1.754
Dihedral 1	-21.75	-10.05
Dihedral 2	1.36	-2.00
MAD	0.011	
MSD	-0.005	
MaxD	0.013	
MinD	-0.115	

Table S1: Bond lengths (Å) and dihedral angles (degree) of **3** optimised at the PCM(DOX)/M06-2X/6-31G(d) level and measured with X-Ray (experimental values from Ref. 1). See Figure S2 for labels. Mean absolute deviation (MAD), mean signed deviation (MSD), and maximum positive and negative deviations (MaxD and MinD) between theoretical and experimental bond lengths are reported at the bottom of the table.

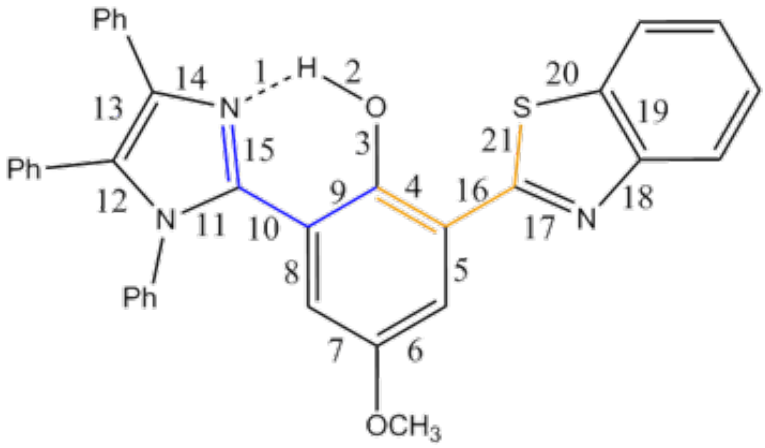

Figure S2: Bond labels of **3** as well as dihedral angle 1 (blue) and 2 (orange).

S2.2 Charge repartition

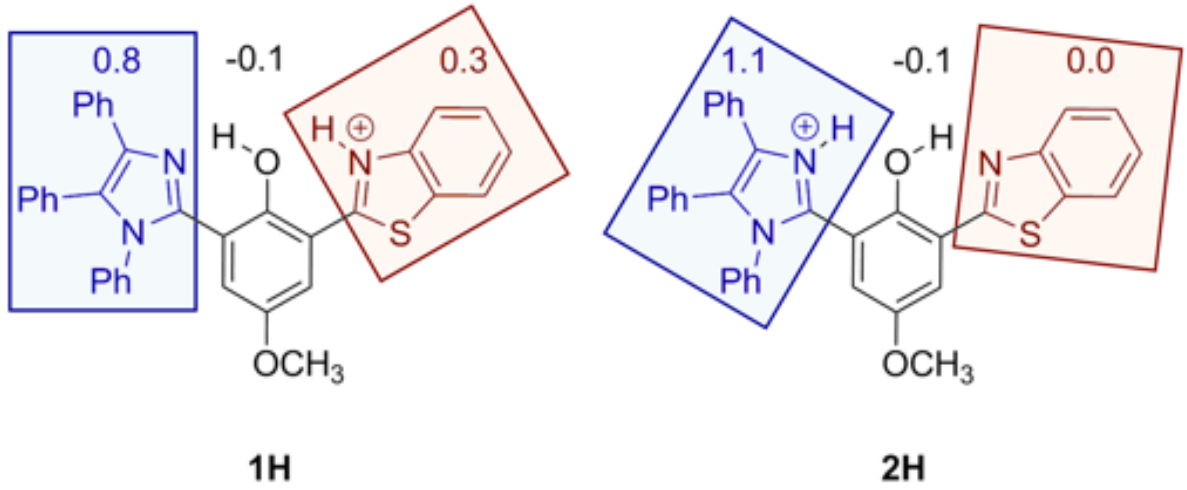

Figure S3: PCM(DOX)-M06-2X/6-311+G(2d,p) repartition of the Mertz-Kollman charge for **1H** and **2H**. In blue, the charge carried by the imidazole part, in black by the phenol moiety and in brown by the benzothiazole group.

	1H				**2H**			
	Ø	BF_4^-	ClO_4^-	Cl	Ø	BF_4^-	ClO_4^-	Cl
Imidazole	0.8	0.7	0.8	0.5	1.1	1.2	0.8	0.9
Benzothiazole	0.3	0.3	0.2	0.3	0.0	0.0	0.1	-0.1
phenol	-0.1	-0.1	-0.1	0.0	-0.1	-0.3	0.0	-0.1
Anion	0.0	-0.9	-0.9	-0.8	0.0	-0.9	-0.9	-0.7
Total	1.0	0.0	0.0	0.0	1.0	0.0	0.0	0.0
	3H				**4H**			
	Ø	BF_4^-	ClO_4^-	Cl	Ø	BF_4^-	ClO_4^-	Cl
Imidazole	1.0	0.0	1.0	0.8	1.1	0.9	0.9	0.9
Benzothiazole	0.1	0.0	0.0	-0.1	0.0	0.0	0.0	0.0
phenol	-0.1	0.0	-0.2	-0.1	-0.1	0.0	0.0	-0.1
Anion	0.0	0.0	-0.8	-0.7	0.0	-0.9	-0.9	-0.8
Total	1.0	0.0	0.0	0.0	1.0	0.0	0.0	0.0
	3H'				**2HH**		**3HH**	
	Ø	BF_4^-	ClO_4^-		Ø	Cl_4^-	Ø	ClO_4^-
Imidazole	0.7	0.6	0.6		1.2	0.9	1.1	1.0
Benzothiazole	0.3	0.3	0.3		0.7	0.6	0.8	0.6
phenol	-0.1	0.0	0.0		0.1	0.2	0.1	0.0
Anion(s)	0.0	-0.9	-0.9		0.0	-1.7	0.0	-1.6
Total	1.0	0.0	0.0		2.0	0.0	2.0	0.0

Table S2: Potential atomic charges determined for various fragments calculated with the Mertz-Kollman model at the PCM(DOX)-M062X/6-311+G(2d,p) level for the $BTImPH^+$ and $BTImPH_2^+$ conformers with and without a counter-anion (two counter-ions for $BTImPH_2^+$).

S2.3 Interaction energies

	BF_4^-	ClO_4^-	Cl^-
1H	-82.01	-76.00	-99.17
2H	-78.18	-76.49	-93.87
3H	-93.20	-89.61	-111.82
4H	-88.80	-85.63	-100.52
3'H	-87.62	-84.28	*
2HH		-119.20	
3HH		-118.08	

$*$: *Calculation of **3'H** with the Cl^- anion in interaction with the benzothiazole moiety did not converge*

Table S3: Complexation energy (kcal/mol) computed at the M06-2X/6-31G(d) level on the PCM(DOX)-M06-2X/6-31G(d) structures. The counterpoise correction was applied. For **2HH** and **3HH**, two counter-ion are included in the system and the total complexation energy divided by two is reported.

S2.4 Representation of the GS of BTImPH$^+$ with and without counter-ion

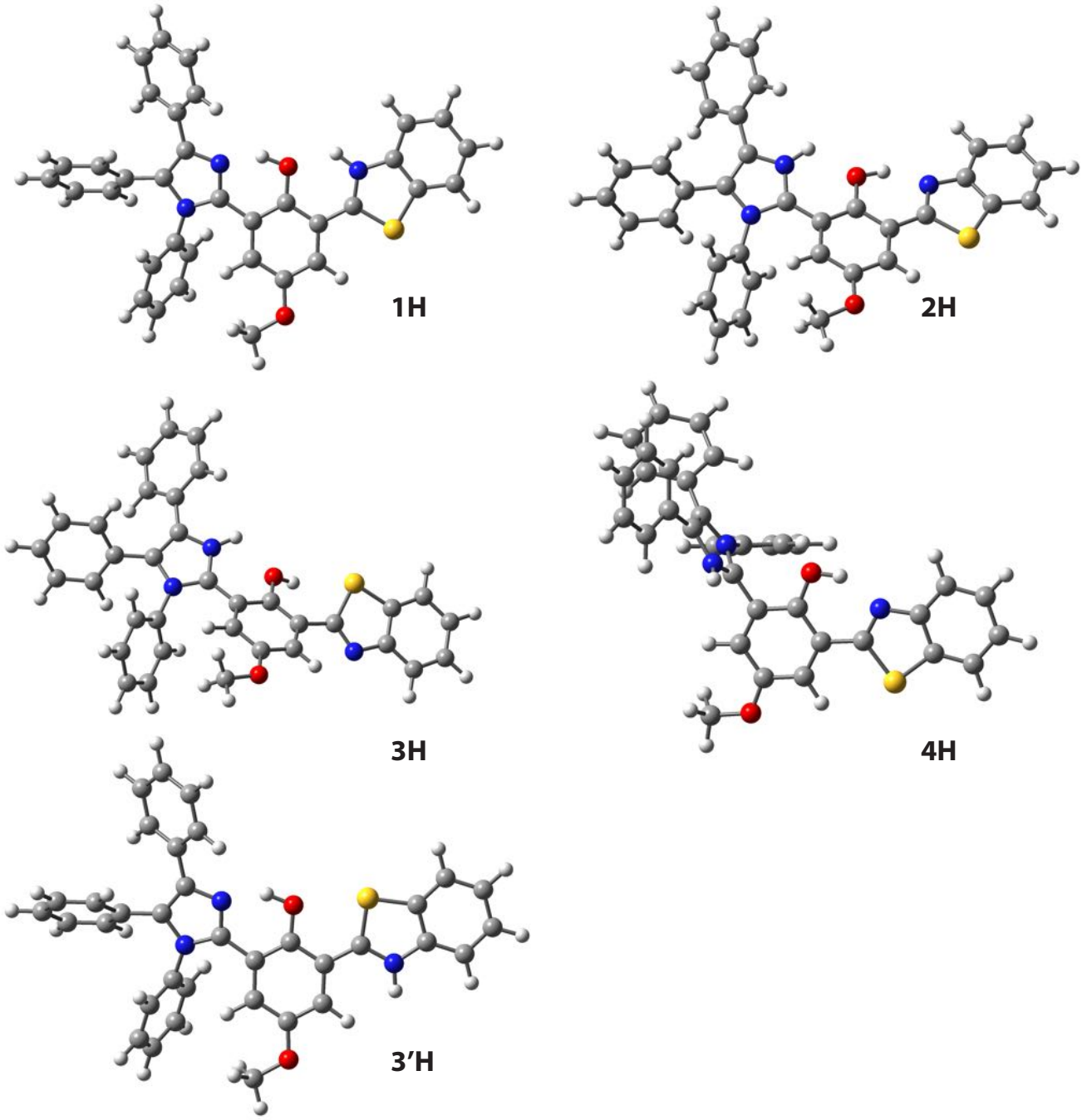

Figure S4: Representation of the optimised ground state of conformers **BTImPH$^+$**.

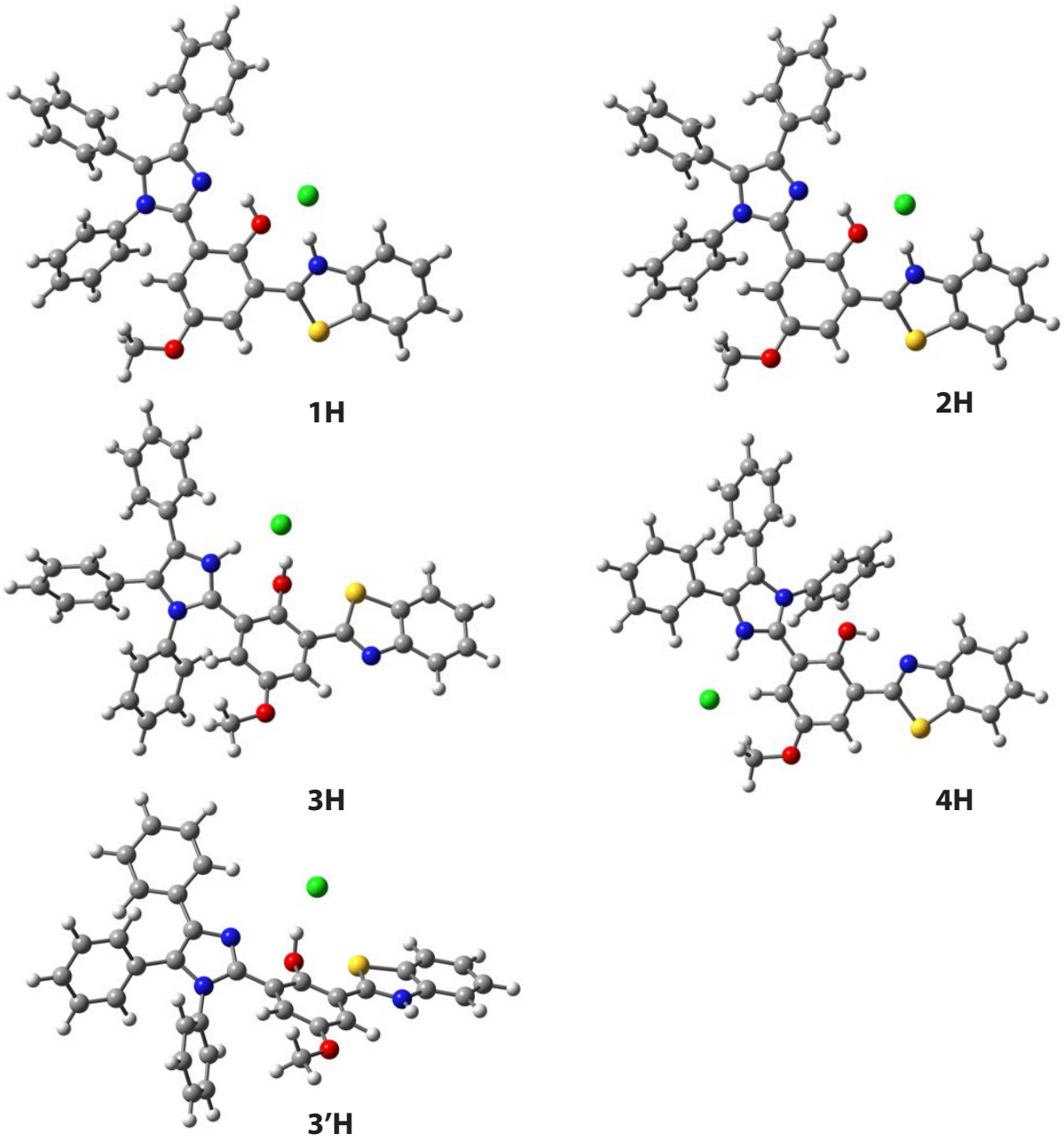

Figure S5: Representation of the optimised ground state of conformers **BTImPH**$^{+}$ with a Cl^{-} counter-ion.

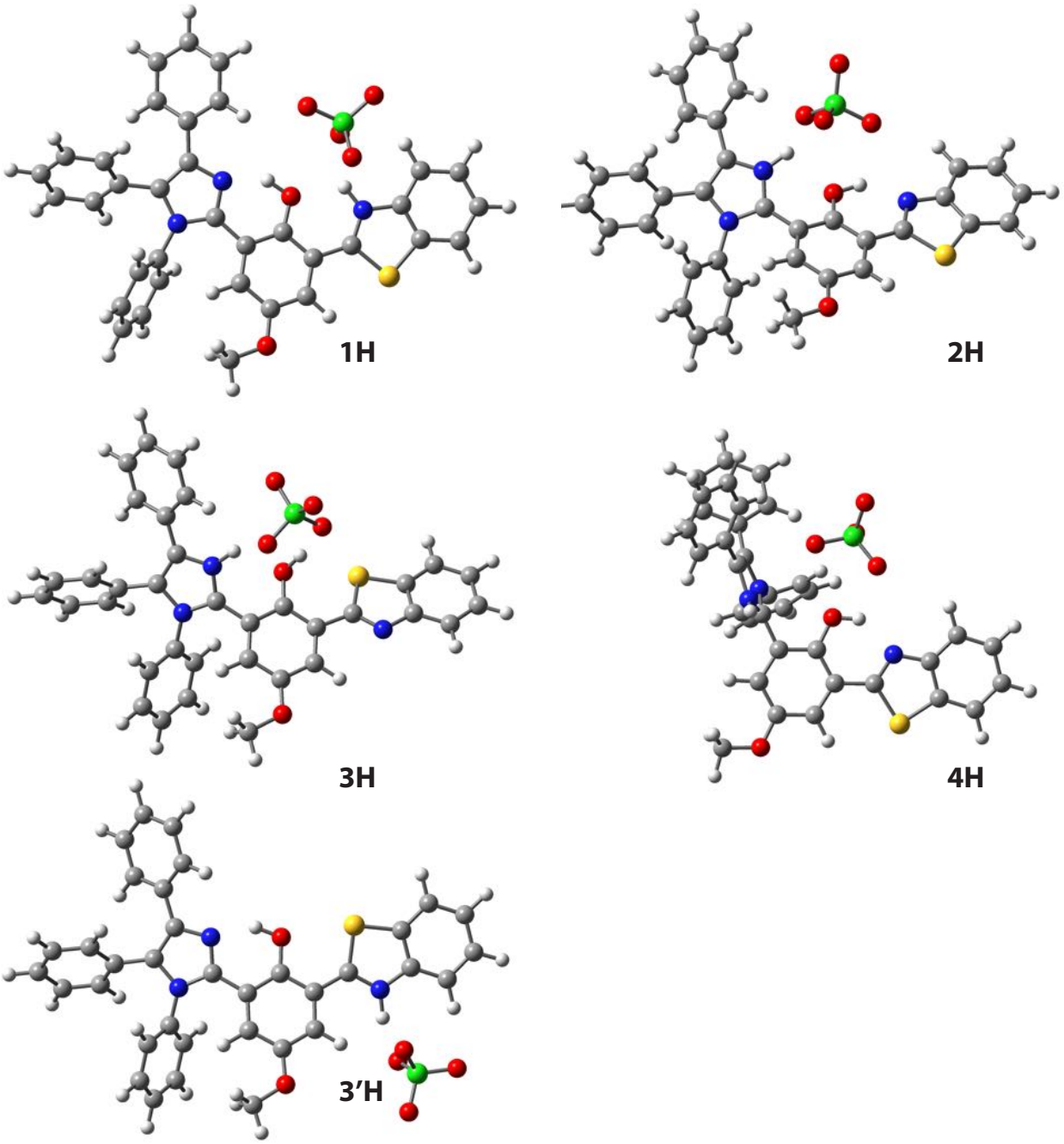

Figure S6: Representation of the optimised ground state of conformers **BTImPH**$^+$ with a ClO_4^- counter-ion.

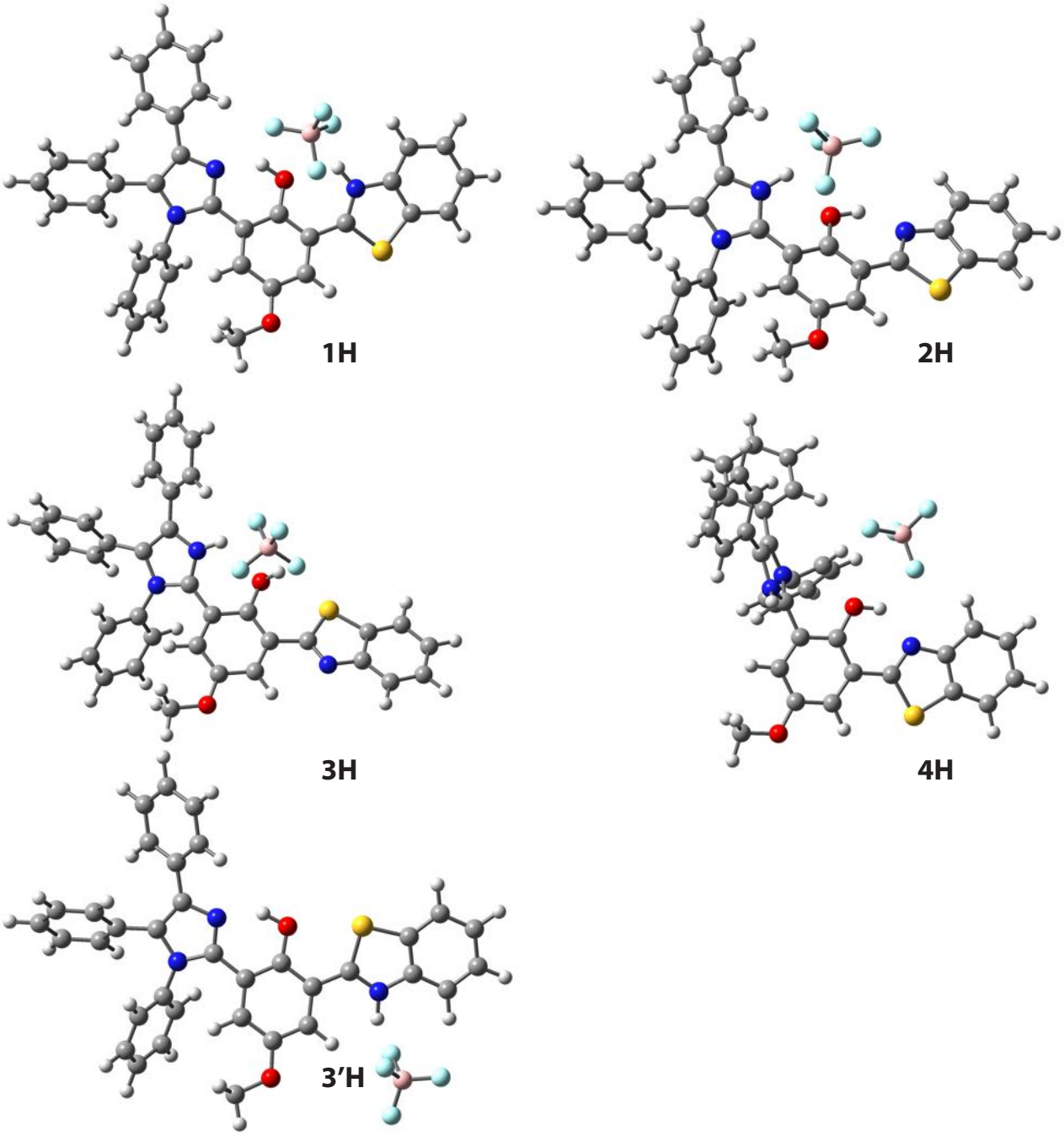

Figure S7: Representation of the optimised ground state of conformers **BTImPH**$^+$ with a BF_4^- counter-ion.

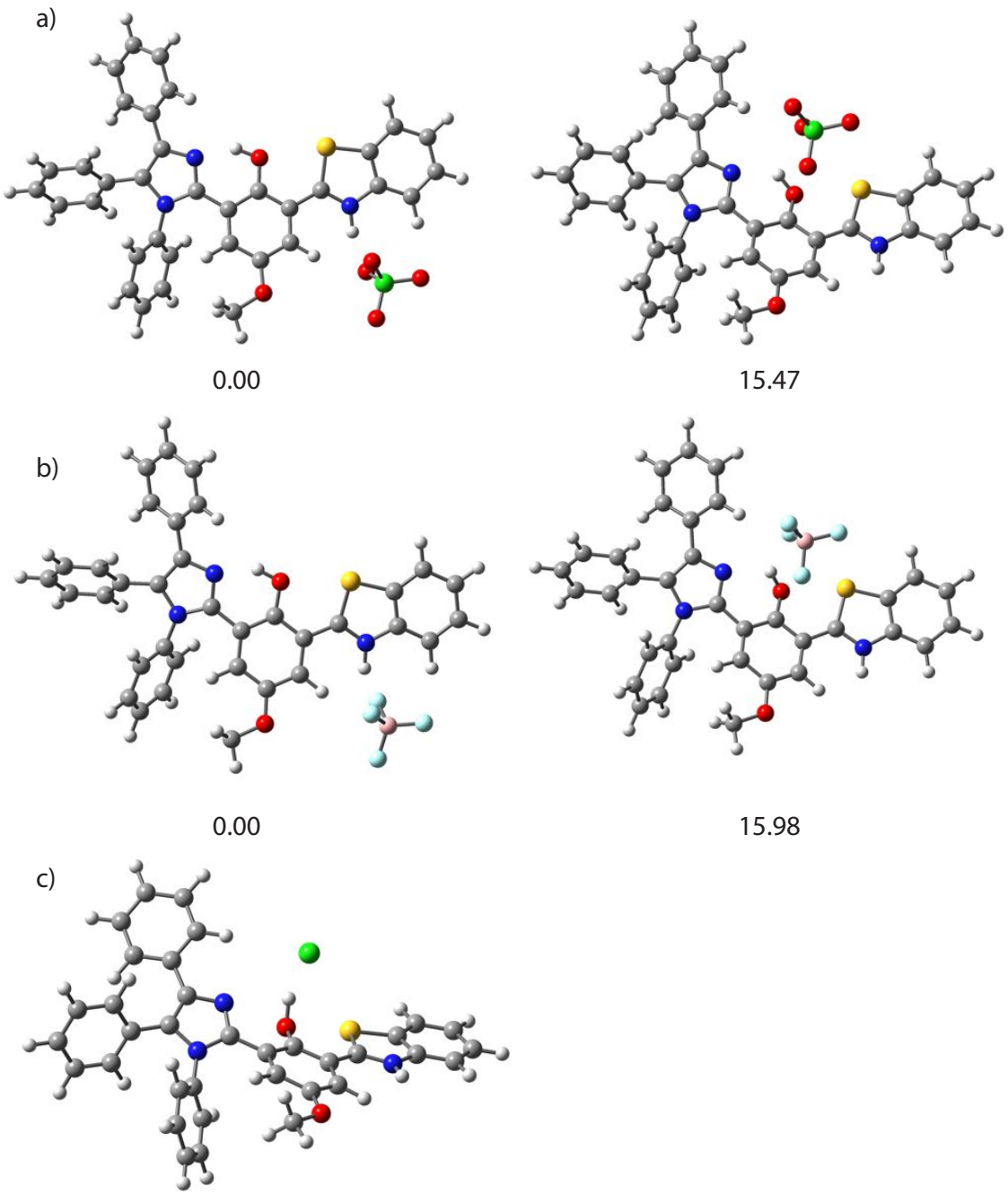

Figure S8: Representation of the optimised ground state of **3'H** with: a) ClO_4^-, b) BF_4^-, and c) Cl^- and relative stability (kcal/mol) depending of the anion location. The optimisation of **3'H** with the Cl^- anion in interaction with the benzothiazole moiety (right structures) did not converged.

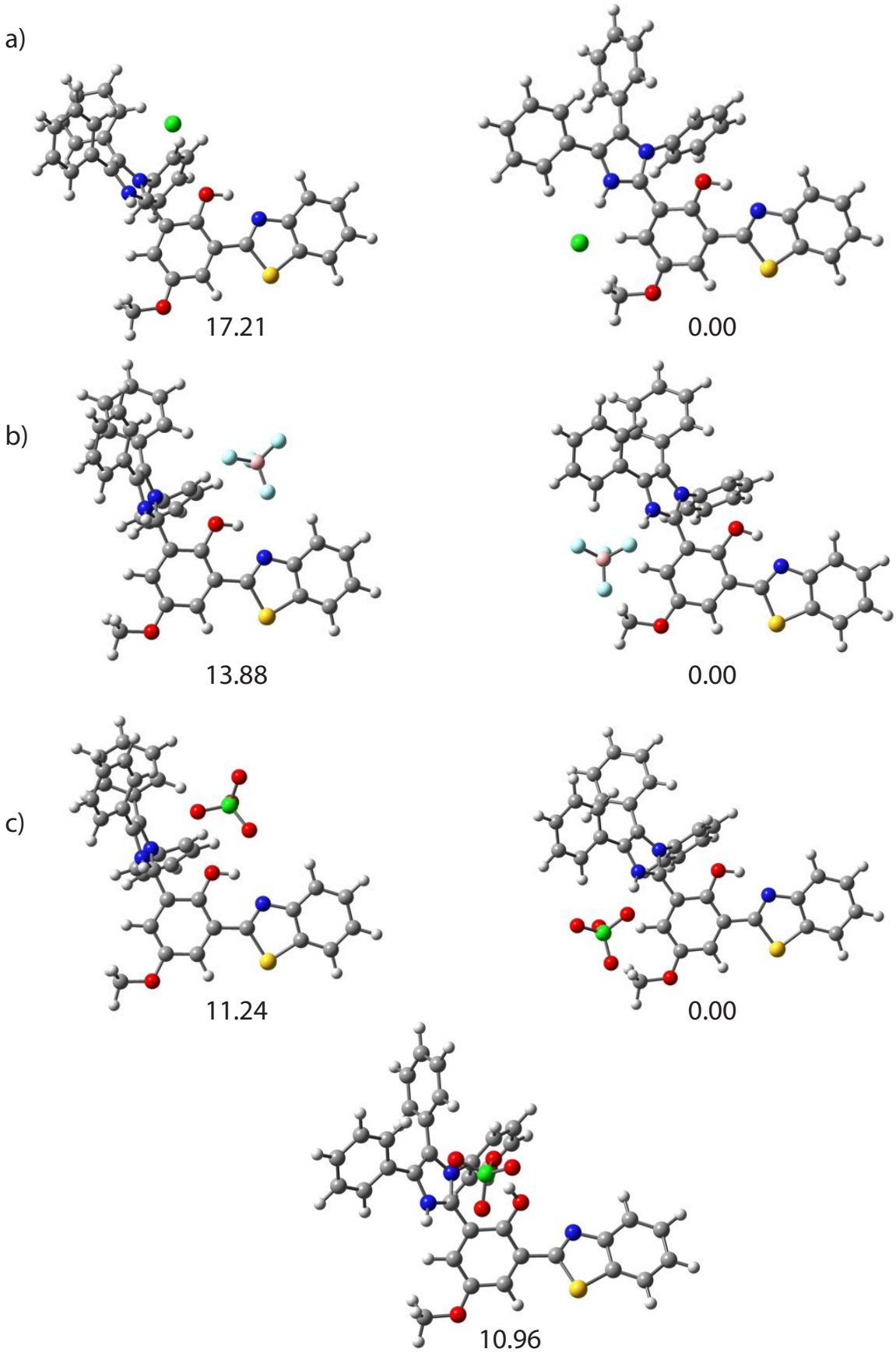

Figure S9: Representation of the ground state optimised structures of **4H** with several counter-ions, a) Cl^{-}, b) BF_4^{-}, and c) ClO_4^{-}, and relative stability (kcal/mol) depending of the anion position.

S2.5 Representation of the GS of $BTImPH_2^+$ in presence or absence of two ClO_4^-

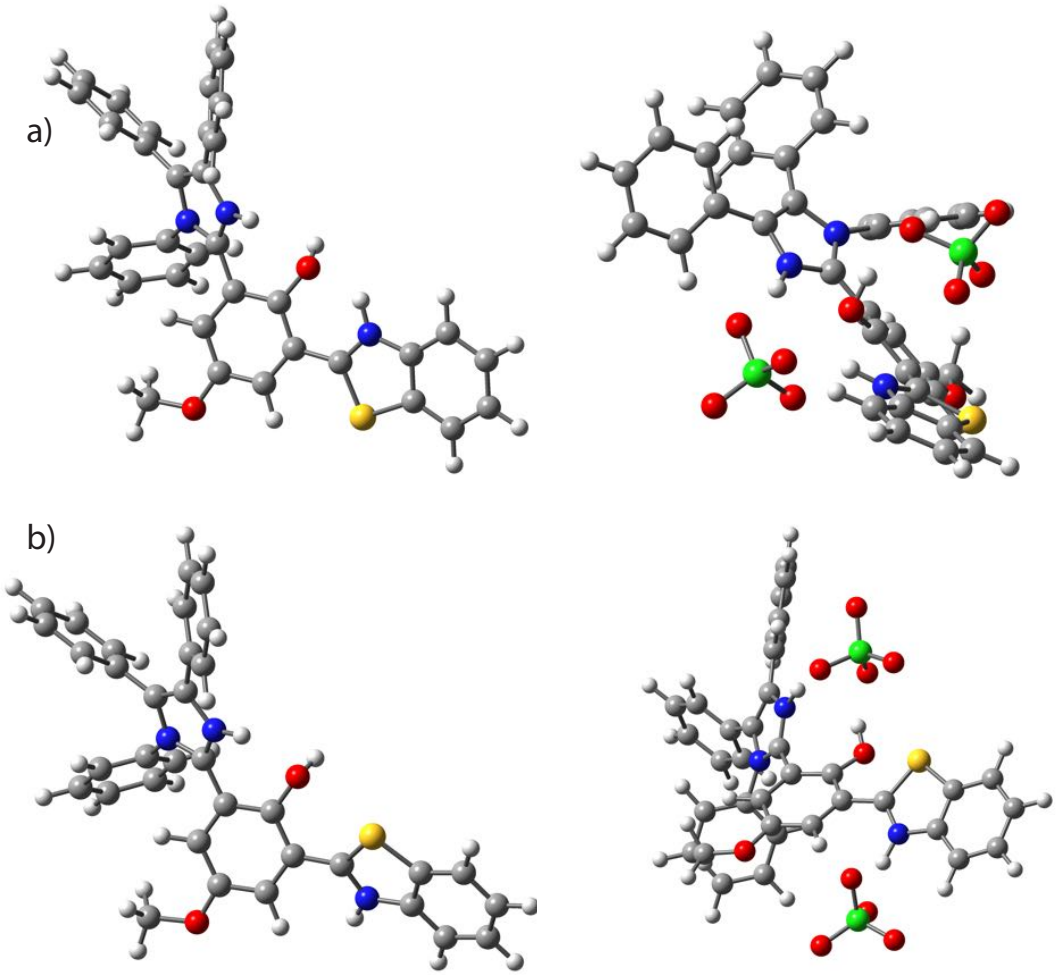

Figure S10: Representation of the optimised ground state of a) **2HH** and b) **3HH** in presence (right) or absence (left) of two ClO_4^- counter-ions.

S2.6 Ground state stabilities of the keto forms of BTImPH$^+$

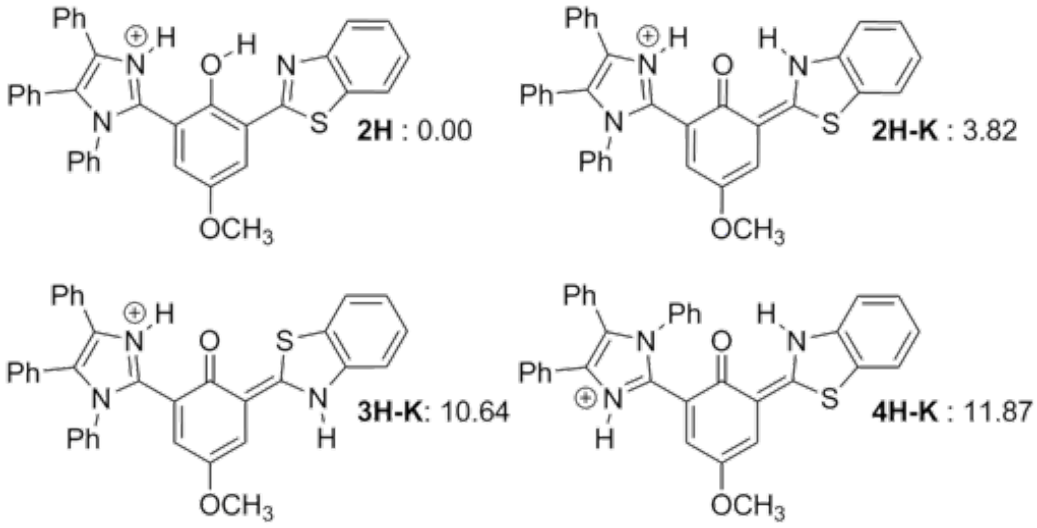

Figure S11: Most stable form (**2H**) and keto conformers of BTImPH$^+$. The relative free energy $\Delta G_{\mathrm{SBS}}^{\mathrm{PCM}}$ in DOX neglecting the counter-ion is indicated in kcal/mol for each structure.

S2.7 NMR

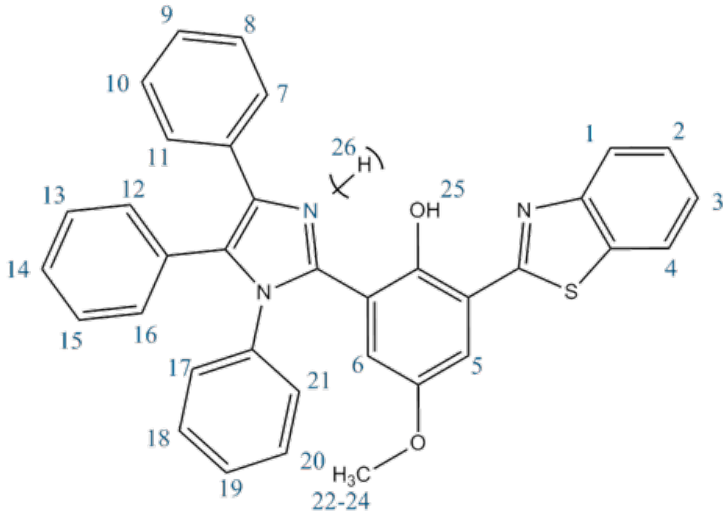

Figure S12: Label of hydrogen atoms used in NMR analysis.

	3	**2H**			**3H**			**4H**		
	∅	∅	BF_4^-	ClO_4^-	∅	BF_4^-	ClO_4^-	∅	BF_4^-	ClO_4^-
H6	6.3	6.4	6.2	6.1	6.4	6.1	6.1	6.8	9.1	9.0
H7	8.6	8.0	9.7	9.3	8.1	8.9	9.1	7.9	9.6	9.4
H1	8.2	8.3	8.2	8.1	8.3	8.3	8.2	8.3	8.2	8.2
H4	8.3	8.3	8.3	8.6	8.5	8.2	8.3	8.3	8.2	8.2
N	249	166	182	181	168	178	179	170	180	181

Table S4: NMR chemical shift (ppm) calculated at the B3LYP/cc-pVTZ level in DOX.

S2.8 absorption

	TD-DFT/LR+cLR				
	2H	**3H**	**4H**	**2HH**	**3HH**
∅	3.55	3.85	3.84	3.56	3.49
BF_4^-	3.55	3.91	3.62		
ClO_4^-	3.59	3.90	3.62	3.67	3.58

Table S5: Absorption energies in eV of the enol ground-state of singly and doubly protonated BTImP without or whitout counter-ion (BF_4^- and ClO_4^-) with DOX solvent at the PCM-M06-2X/6-311+G(2d,p) level. The reported experimental absorption maxima are 3.25 eV (blue) and 3.33 (red) eV in Ref. 2

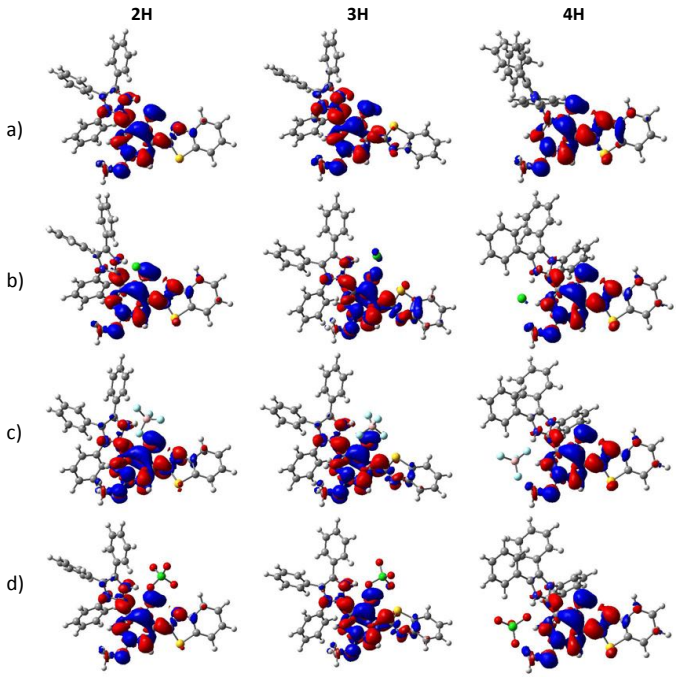

Figure S13: Electron density difference between ES and GS (isovalue = 0.001 a.u.) of $BTImPH^+$ calculated with M06-2X/6-31G(d) in DOX, a) without anion, b) with Cl^-,and c) BF_4^-. Blue (red) regions indicate decrease (increase) of the density upon absorption of light.

S2.9 Emission

				$\emptyset$	
	2H	**3H**	**4H**	**2HH**	**4HH**
E*	3.12	3.22	[a]	2.92	2.45
K*	2.33	/	2.28	/	/
				BF_4^-	
	2H	**3H**	**4H**	**2HH**	**4HH**
E*	2.91	3.18	[a]	/	/
K*	2.20	/	2.24	/	/

a: E optimisation could not converge properly and leads to a K**

Table S6: Emission energies (E* and K*) in eV of singly and doubly protonated BTImP in presence or absence of BF_4^- counter-ion at PCM(DOX)-M06-2X/6-311+G(2d,p) level with the LR+cLR solvation model.

S3 Results of calculations performed in tetrahydrofuran

S3.1 Relative stability of conformers in ground-state

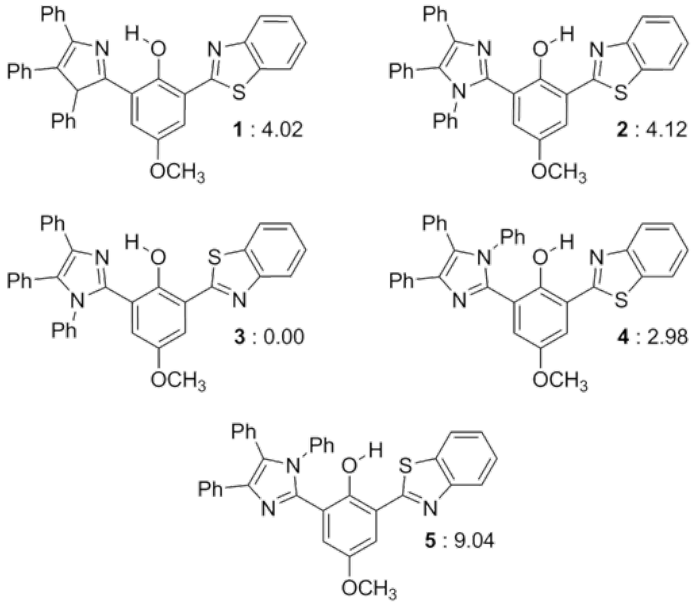

Figure S14: Relative free energy in kcal/mol of the BTImP conformers calculated in THF at the M06-2X/6-31G(d) level.

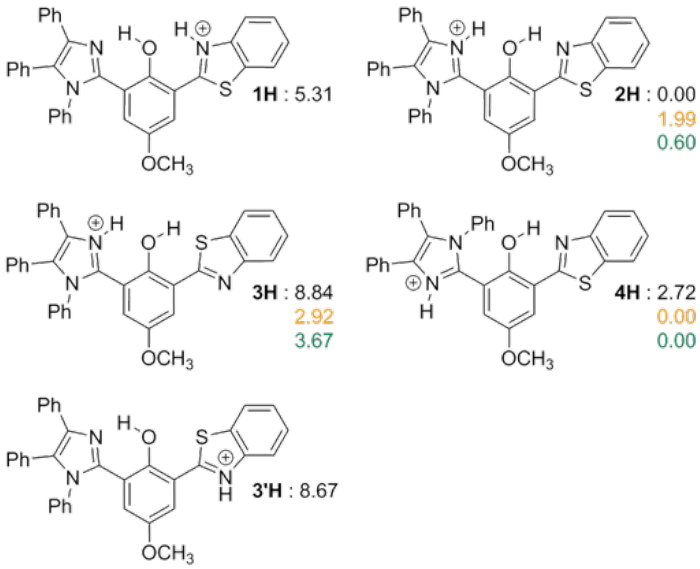

Figure S15: Protonated BTImP conformers. Relative free energy in THF in kcal/mol; without anion (black), with BF_4^- (orange), and with ClO_4^- (green). The counter-ion is located near the formal positive charge, see Figures S2-S7.

S3.2 NMR

	2H	**3H**	**4H**
H6	-0.1	-0.1	2.4
H7	0.9	0.2	0.8
H1	0.0	0.0	-0.1
H4	0.0	0.1	-0.1
N	-64	-67	-71

Table S7: Difference of NMR chemical shift (ppm) between BTImP and its protonated form in THF calculated with B3LYP/cc-pVTZ and experimentally measured.[2]

	2H			**3H**			**4H**		
	$\emptyset$	BF_4^-	ClO_4^-	$\emptyset$	BF_4^-	ClO_4^-	$\emptyset$	BF_4^-	ClO_4^-
H6	6.5	6.3	6.3	6.4	6.3	6.3	6.9	8.8	8.7
H7	8.1	9.4	8.9	8.1	8.7	8.9	8.0	9.3	9.2
H1	8.3	8.3	8.3	8.3	8.3	8.3	8.3	8.2	8.2
H4	8.3	8.3	8.5	8.4	8.4	8.4	8.3	8.2	8.3
N	161	178	178	163	175	176	165	171	178

Table S8: NMR chemical shift (ppm) calculated with B3LYP/cc-pVTZ in THF for $BTImPH^+$ in presence and absence of counter-ion

S3.3 Optical properties

	$\Delta G_{\mathrm{LBS}}^{\mathrm{cLR}}$	$\Delta G_{\mathrm{LBS}}^{\mathrm{LR+cLR}}$
$E^* \rightarrow K^*$	-5.37	-6.14
$E^* \rightarrow TS^*$	-1.05	-1.25

Table S9: Difference of free energy (in kcal/mol) between E^*, K^*, TS^*, and $TS2^*$ for **3** calculated at the TD-M06-2X/6-311+G(2d,p) level in THF.

	ΔE_{cLR}	$\Delta E_{\mathrm{LR+cLR}}$	Exp
E	3.70	3.66	3.28
E^*	3.20	3.03	
K^*	2.56	2.42	2.29

Table S10: Absoprtion (E) and emission (E^* and K^*) energies in eV of **3** obtained at the M06-2X/6-311+G(2d,p) level in THF using the non-equilibrium PCM limit. Experimental data are taken from Ref 1.

References

[1] K.-i. Sakai, S. Tsuchiya, T. Kikuchi and T. Akutagawa, *J. Mater. Chem. C*, 2016, **4**, 2011–2016.

[2] S. Tsuchiya, K.-i. Sakai, K. Kawano, Y. Nakane, T. Kikuchi and T. Akutagawa, *Chem. Eu. J.*, 2018, **24**, 5868–5875.